Journal of Atmospheric and Solar-Terrestrial Physics 112 (2014) 47–56

Contents lists available at ScienceDirect

Journal of Atmospheric and Solar-Terrestrial Physics

journal homepage: www.elsevier.com/locate/jastp

Global and direct UV irradiance variation in the Nahuel Huapi National Park (Patagonia, Argentina) after the eruption of Puyehue-Cordon Caulle (Chile)

S.B. Diaz [a,*], A.A. Paladini [b], H.G. Braile [c], M.C. Dieguez [d], G.A. Deferrari [e], M. Vernet [f], J. Vrsalovic [e]

[a] INGEBI/CADIC/CONICET, Vuelta de Obligado 2490, 1428 Buenos Aires, Argentina
[b] INGEBI/CONICET, Vuelta de Obligado 2490, 1428 Buenos Aires, Argentina
[c] INGEBI/ANPCyT, Vuelta de Obligado 2490, 1428 Buenos Aires, Argentina
[d] INIBIOMA, UNC, San Carlos de Bariloche, 8400 Neuquen, Argentina.
[e] CADIC/CONICET, B. Houssay 200, 9410 Ushuaia, T. Del Fuego, Argentina
[f] Scripps Institution of Oceanography, University of California San Diego, La Jolla, CA 92093-0218, USA

ARTICLE INFO

Article history:
Received 14 September 2013
Received in revised form
6 February 2014
Accepted 25 February 2014
Available online 12 March 2014

Keywords:
UV radiation
Global irradiance
Direct irradiance
Volcanic eruptions

ABSTRACT

On June 4th, 2011, the Puyehue-Cordon Caulle volcanic complex (40°35′25″S 72°07′02″W, Chile) started eruption, sending ash 45,000 feet into the atmosphere. After the initial period, the eruption continued for several months, with less intensity. Changes in global irradiance in the UV-B and UV-A, and direct irradiance and AOD in the UV-A, as consequence of the eruption, were studied. Global irradiance has been permanently measured at the Laboratory of Photobiology (LPh) (41.13S, 71.42W, 804 msl) since 1998. In addition, in the frame of a project to study altitude effect on direct and global irradiance, field campaigns were performed during September 17th to 23rd, 2010 and September 14th to 18th, 2011, in the region of the Nahuel Huapi National Park, near 100 km from the eruption. In those periods, simultaneous measurements of direct and global irradiance and aerosol optical depth (AOD) were carried out at three sites: Laboratory of Photobiology (LPh), Mt Otto (41.15S, 71.38W, 1386 msl) and Mt Catedral (41.17S, 71.48W, 1930 msl). The analysis of aerosols in 2011, three to four month after the eruption started, showed the presence of larger particles and more variability than in 2010, at all sites. Global irradiance, at LPh, also exhibited larger variability, compared to 1999, when no eruption or any other event that could have produced major changes in aerosols occurred. The mean decrease, as consequence of the volcano activity, at LPh, was around 20%, at 305 nm and closed to 10%, at 320 nm. At 380 nm, the decrease was very small and not statistically significant, although in particular days, with large aerosol load, a significant decrease was observed. Direct irradiance, in the UV-A, showed larger decrease than global irradiance. The effect of the eruption was more pronounced at the low altitude site.

1. Introduction

When trespassing the atmosphere and reflecting on the ground, solar ultraviolet (UV) radiation is affected by scattering and absorption processes. Sun-Earth distance, atmospheric gases and aerosols, solar zenith angle (SZA), clouds and surface albedo are the main factors that determine ground-level radiation. The dependence of irradiance on some of these parameters is well established (i.e.: SZA and sun-Earth distance), others present seasonal and geographical variations (i.e.: Total Ozone Column) (Chubarova et al., 1997; Díaz et al., 1994; Frederick et al., 1994; Lubin and Frederick, 1989) and others are not easy to predict (i.e.: clouds) (Chubarova et al., 1997; Estupinan et al., 1996; Frederick and Steele, 1995).

The effect of atmospheric aerosols on surface UV radiation is important and depends on the total atmospheric loading and their optical and microphysical properties. Large differences have been observed in irradiance between urban and rural locations, or between rather polluted sites in the Northern Hemisphere and cleaner sites in the Southern Hemisphere. McKenzie et al. (2006) observed that, as consequence of aerosol differences, the UV Index peak values were approximately 40% larger at 45°S in New Zealand, than those at 45°N in North America. Ground-based measurements have shown that large reductions in the UV-B

* Corresponding author. Tel.: +54 11 4783 2871.
E-mail address: diazsusanab@gmail.com (S.B. Diaz).

http://dx.doi.org/10.1016/j.jastp.2014.02.006
1364-6826

occurred under the effect of absorbing aerosols such as smoke from biomass burning (Kirchhoff et al., 2001), forest fires (McArthur et al., 1999), or desert dust (di Sarra et al., 2002).

Aerosols loading and size distribution are largely modified by volcanic eruptions. They inject ash and non-ash particles (sulfate) into the atmosphere, affecting regional Aerosols Optical Depth (AOD) (Ansmann et al., 2011). In the case of major eruptions, these particles can last for long periods even at sites far away from the emission source (Michalsky et al., 2010; Skouratov, 1997). Ash particles contribute to the coarse mode fraction, while sulfate particles are comparatively smaller and thus belong to the fine particle mode (Ansmann et al., 2011). It has been observed that the increase of SO_2 over areas affected by high volcanic activity or over regions close to coal burning industries, may result in approximately 2% attenuation of erythemal irradiance and, at some UV wavelengths, the reduction can exceed 20% (McKenzie et al., 2008).

A layer of sulfuric acid aerosol is present in the lower stratosphere, at all latitudes. During "background" conditions (volcanically quiescent periods), the dominant source of this aerosol layer is thought to be the photolysis of carbonyl sulfide and sulfur entering the stratosphere in the form of sulfur dioxide (SO_2) (SPARC (Stratospheric Processes And their Role in Climate), 2006, Bekki and Bodeker, 2010). The other major source of sulfur to the stratosphere is volcanoes activity. Major volcanic eruptions can inject large amounts of this element directly into the stratosphere, increasing the stratospheric aerosol layer for several years, as observed after the eruptions of El Chichón in 1982 and Mt. Pinatubo in 1991.

After a period of low activity, on June 4th, 2011, a fissure opened in the Puyehue-Cordon Caulle volcanic complex (40°35′25″S 72°07′02″W, Chile) (Fig. 1), sending ash 45,000 feet into the atmosphere (NASA, 2013a,b; SERNAGEOMIN, 2013). The Cordón Caulle is one of the most active in Southern Andes and the previous event was in 1960. In this event as well as in the most recent of 2011, the eruption occurred through a fissure in the section of the Cordón Caulle while the stratocone of the Puyehue volcano remained dormant. During the eruption of 2011, ash, sand and pumice were ejected and the ash emission was blown east. Heavier material was falling out of the ash cloud and finer particles remained suspended in the atmosphere. Near the town of San Carlos de Bariloche, a layer of material around 30 cm deep covered the ground. As the eruption continued, the plume traveled east, and reached the Atlantic Ocean, forcing flight cancellations at several airports and affecting different downwind regions of the Southern Hemisphere around the world, for a few months (NASA, 2013a,b; SERNAGEOMIN, 2013). In September 2011, the airport of San Carlos de Bariloche was still not operative.

Several NASA satellites have captured images of the ash plume. One of the instruments that provided daily imagery of the plume was the MODIS (Moderate Resolution Imaging Spectroradiometer), Terra and Aqua satellites (NASA, 2013a,b). Fig. 2a shows an image for June 6th, a couple of days after the eruption began. The activity continued for several months, with a plume much smaller than during the opening phase, as can be seen in Fig. 2b and c, which correspond to September 17th and November 16th, respectively. During this period, high atmospheric winds were carrying the ash away and, depending on wind intensity, it was carried as much as 120–250 km from the vent.

In this paper, we analyzed the effect of this eruption on direct and global UV irradiance at sites located at different altitudes inside Nahuel Huapi National Park (NHNP) (Fig. 1).

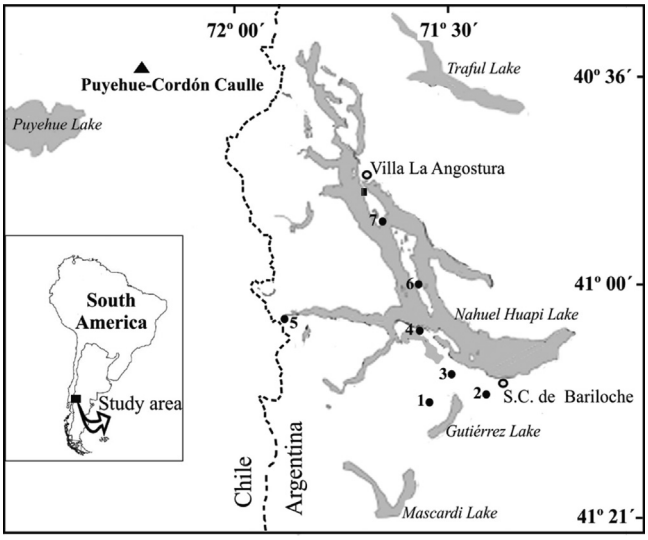

Fig. 1. Puyehue-Cordon Caulle and Nahuel Huapi National Park (NHNP) area: (1) Mt Catedral, (2) Mt Otto, (3) Laboratory 1 of Photobioloy, (4) 2 Port Pañuelo and San Eduardo Chapel, (5) Port Blest, (6) Victoria Island – Port 3 Anchorena and (7) Quetrihue Penninsula – Arrayanes Forest.

2. Data and methodology

Global irradiance has been permanently measured at the Laboratory of Photobiology (LPh), INIBIOMA, Universidad Nacional del Comahue (LPh) (41.13S, 71.42W, 804 msl) since 1998. Measurements performed during 2011, before and after the eruption, and in 1999, as reference year, were used in order to determine the effect of the volcano on global irradiance.

Fig. 2. MODIS images for the eruption of the Puyehue-Cordon Caulle volcanic complex: (a) June 6th, 2011 (NASA Goddard/MODIS Rapid Response Team) and (b) September 17th (NASA image courtesy Jeff Schmaltz MODIS Rapid Response Team, NASA-GSFC), (c) November 16th (NASA image courtesy Jeff Schmaltz, LANCE/EOSDIS MODIS Rapid Response Team at NASA GSFC).

Table 1
Sites and periods used, for each of the parameters, in this analysis.

Site	Global irradiance	Direct irradiance and AOD
Lab. of Photobiology (LPh)	Mar 15th to Oct 18th 2011 Mar15th to Oct 18th 1999	Sep 14th to 18th, 2011 Sep 17th to 23rd, 2010
Mt Otto and Mt Catedral (alternating)	Sep 14th to 18th, 2011 Sep 17th to 23rd, 2010	Sep 14th to 18th, 2011 Sep 17th to 23rd, 2010

In addition, field campaigns were performed during September 17th to 23rd, 2010 and September 14th to 18th, 2011, in the region of the NHNP (Fig. 1), in the frame of a project to study altitude effect on direct and global irradiance at the Andes, Simultaneous measurements of direct and global narrow band irradiance and aerosol optical depth (AOD) were carried out at the Laboratory of Photobiology (LPh), and at a mobile station, which alternated between Mt Otto (41.15S, 71.38W, 1386 msl) and Mt Catedral (41.17S, 71.48W, 1930 msl). Table 1 summarizes the data used at each site.

Although the results obtained during the campaigns derived from a small number of days, we included them in this paper, because they were consistent with the results obtained from the much larger sample for global irradiance, at LPh. Also, they provided a broader vision of the situation, adding more parameters (direct radiation, AOD and Angstrom exponent) and sites at different altitudes.

The town of San Carlos de Bariloche (80,000 inhabitants, ~20,000 ha) is included in the Nahuel Huapi National Park (NHNP) (Fig. 1). The city is surrounded by a mixed Nothofagus forest. The snow covers the surface during part of the winter and the weather is highly variable due to the strong westerly winds. The Laboratory of Photobiology (LPh) is located at the west of San Carlos de Bariloche, on a derivation of the road to Catedral Village. The place is surrounded by a planted field of non-native pine tree species that is spotted with native trees and shrubs. The site lacks neighbors, except for a small research laboratory. Mt Otto is situated at ~4 km southwest from the city. It is a tourist point with a lift that reaches the top at 1386 msl, where the measurements were performed. Mt Catedral is a ski resort, and the measurements were done at a station set up at Mountain Refuge Lynch, located at 1930 msl. During September of 2010 and 2011, the snow was present at all the sites; however the snowpack was lower at lower altitudes. Aerosols in this type of locations are likely biogenic, contributed by the forest and soil.

2.1. Global irradiance

Global irradiance was measured with two multi-channel radiometers. A GUV 511 (Biospherical Instruments Inc.) was used to collect data at the fix station (LPh), while a BIC 250 (Biospherical Instruments Inc.) served at the mobile stations (Mt Otto and Mt Catedral).

The GUV 511 is a temperature stabilized multi-channel radiometer, which measures down-welling irradiances with moderately narrow bandwidth channels (near 10 nm), centred at, approximately, 305, 320, 340 and 380 nm, plus PAR (400–700 nm) (Booth et al., 1994). The radiometer has been periodically sun calibrated with a reference GUV (RGUV) (Diaz et al., 2006) and during the field campaign 2011 as well, following the procedure described by Diaz et al. (2005).

The radiometer BIC 250 is also a multi-channel radiometer (305, 320 and 380 nm, approx. 10 nm bandwidth), similar to the GUV 511, except that it is not stabilized in temperature and is not provided with the 340 nm and PAR channels. A correction for temperature changes was applied to the calibration constants according to Booth (1998). This radiometer was calibrated against the reference instrument (RGUV) and inter-compared with the GUV 511 sited at the LPh (September 14th, 2011). Due to instruments malfunction, values for channel 380 nm of the BIC were derived from the other channels, following a multi-regressive procedure (Díaz et al., 2003).

Global irradiance was provided at 1 min intervals. Dark values (instrument internal noise) for the GUV were obtained from night values (Diaz et al., 2006). For the BIC, they were obtained covering the collector during 5 min, at the beginning and end of daily measurements. Daily, the collectors were cleaned and the instruments were levelled to $\leq 0.1^{\circ}$, in direction North–South and East–West.

At LPh, data from year 2011, which included the days of the 2011 campaign, was used to analyze global irradiance variations. Clear sky global irradiance at 305, 320 and 380 nm was considered in the analysis. Days that were most of the time clear were selected. Small periods with cloudy sky were removed, and then, data was daily fitted with a sixth degree polynomial, at 305 nm, and a fourth degree polynomial, at 320 and 380 nm. In order to compare different days and years, the values were corrected by sun-Earth distance and grouped at 1° Solar Zenith Angles (SZA) intervals. Then, days before and after June 4th were grouped, calculating mean and standard deviations at 1° SZA interval. The total number of clear days was 32 (20 before the eruption and 12 after). Clear days resulted to be distributed between March 15th and May 6th, and September 15th and October 18th. Since clear sky days were not available closer to the beginning of the eruption, the results obtained in this analysis reflected the situation three to four months after the eruption started, but while the volcano was still active, as shown in Fig. 2. As a reference for global irradiance at LPh, year 1999 was chosen, when no eruption or any other event that would have produced major changes in AOD was present. The total number of clear sky days, for 1999, was 18 (8 before and 10 after June 4th). Data for 1999 was processed as explained for 2011.

At 380 and 320 nm, once probed that the effect of albedo changes was negligible (see Section 3), the variation observed between global irradiance measured before and after the eruption was considered a consequence of aerosol changes mainly due to the eruption, but, at 305 nm, the effect of total ozone column (TOC) changes should also be taken into account. Then, to determine the contribution of the eruption at 305 nm, at the fix station, days with equal or very closed TOC were compared. In addition, with the aims of obtaining a larger sample, we modeled global irradiance, at SZA 45, 50 55 and 60°, for the identified clear days between March 15 and October 18th, 2011. For this purpose, we used a disort model (Stamnes et al., 1990), applying as input the corresponding total ozone column and aerosol load equal zero. Comparing the modeled values for days after eruption and days before the eruption, at the same SZA, we obtained the difference in irradiance only as consequence of ozone changes.

$$\Delta Irr_{Oz} = (I_{0i} - I_{0j})/I_{0j} \quad (1)$$

where ΔIrr_{Oz} is difference in modeled global irradiance due to ozone changes, I_{0i} is modeled irradiance for day i, after the eruption, $i=1$ to m, and I_{0j} is modeled irradiance for day j, before the eruption, $j=1$ to n, in both cases calculated with aerosol load equal zero.

Also, comparing the actual measured values after and before the eruption, at the same SZA

$$\Delta Irr_{Oz+AOD} = (I_i - I_j)/I_j \quad (2)$$

where ΔIrr_{Oz+AOD} is difference in measured global irradiance due to ozone and aerosols changes, I_i is measured irradiance at day i, after the eruption, $i=1$ to m, and I_j is measured irradiance at day j, before the eruption, $j=1$ to n.

Then, the irradiance variation due to the volcano eruption is the difference between 2 and 1,:

$$\Delta Irr_{AOD} = \Delta Irr_{Oz+AOD} - \Delta Irr_{Oz} \quad (3)$$

This procedure was also applied when analyzing 1999 and when comparing global irradiance, in the mobile stations, during the campaigns 2010 and 2011.

For the mobile stations, changes in global irradiance, as consequence of the volcano eruption, were determined comparing clear sky data for the campaigns 2010 and 2011. The campaigns were performed between September 17th to 23rd, 2010 and September 14th to 18th, 2011. From those days, only September 20th, 22nd and 23rd, 2010 and September 16th, 17th and 18th, 2011 presented clear skies. Same corrections and data fittings were used as explained for LPh global irradiance.

Comparison of global irradiance at both campaigns could not be performed at LPh, since data for global irradiance campaign September 2010 was lost, as consequence of a computer failure.

Total ozone column used in this paper was obtained from OMI instrument (KNMI/NASA) on board the Aura satellite, version 8.5 (Mc Peters and Beach, 2013). When this data was not available, ozone was calculated from global irradiance, following the procedure described in Dahlback (1996).

2.2. AOD and direct irradiance

Aerosols optical depth (AOD) and direct irradiance were measured by two handheld Microtops II sun-photometers (Solar Light Company Inc.) (Morys et al., 2001). One of the instruments was operated at the LPh and the other at the mobile station. These instruments measured direct solar irradiance with an angle of view of 2.5° at 340, 380, 500, 936 and 1020 nm, deriving the AOD for each of those bands. In this study results for 380 nm were presented (380 ± 0.4 nm, 4 nm FWHM). The instruments were factory calibrated (Solar Light Co, Glenside) in August 2009 and December 2012. The calibrations were performed with reference sunphotometers calibrated at Mauna Load Observatory by Langley plot method. In addition, the Microtops II were calibrated using Langley technique, in August 2011, at Tilcara (23.58S, 65.40W, 2492 msl), which is a very clean site with predominance of clear skies, located at the Puna (Andinean Northwest region of Argentina). The change of the direct irradiance constants and the extraterrestrial voltage, between calibrations, was smaller than 3%. For AOD, 1% change for the extraterrestrial voltage corresponds to a change of 0.01, at airmass 1.0, The change in AOD, with respect to percent change in extraterrestrial voltage decreases with increasing airmass.

For the fix station, as well as for the mobile, changes in direct irradiance and AOD, as consequence of the volcano eruption, were determined comparing data for September 2010 and 2011, taking values for 2010 as typical for the time and sites under study. Microtops II provides AOD at 380 and 340 nm (both at the UV/A). Since both wavelengths showed similar results and only global irradiance at 380 nm was available at the mobile station, only AOD and direct irradiance at 380 nm were included in the analysis. These parameters were measured every 20 min, if a clean direct sun observation was possible. Otherwise, the measurements were performed as often as possible. In order to compare different sites and years, direct irradiance, at 380 nm, was calculated each 1 min by fitting the measured clear sky values with a 4th degree polynomial (Diaz et al., 2013), and corrected by sun-Earth distance. Data was then grouped at 1° SZA.

In addition to AOD, aerosols were also analyzed calculating the Angstrom exponent (Angstrom, 1929). It is defined as the slope of the natural logarithm of AOD as a function of the natural logarithm of the wavelength and characterizes the wavelength dependence of AOD. The Angstrom exponent is also a qualitative indicator of aerosol particle size (Angstrom, 1929). Values of the exponent minor or equal to 1 indicate size distributions dominated by coarse mode aerosols (radii ≥ 0.5 μm) and values above 2 indicate size distributions dominated by fine mode aerosols. (radii < 0.5 μm) (Eck et al., 1999).

In order to evaluate the differences in the type of aerosols present in September 2010 and 2011, we calculated the Angstrom exponent applying least squares to the exponents obtained from AOD at the wavelength pairs 380–340 nm, 500–380 nm and 1020–500 nm (Eck et al., 1999)

$$\alpha = -\frac{In\,[\tau_{a_2}/\tau_{a_1}]}{In\,[\lambda_2/\lambda_1]} \quad (4)$$

where α is the Angstrom exponent, $\tau_{a_{1,2}}$ is the AOD at wavelength 1 and 2 and $\lambda_{1,2}$ are wavelengths 1 and 2.

Usually, the function ln AOD versus ln λ is not linear, since the value of α depends on the pair of wavelength selected. Eck et al. (1999) have shown that the relation between ln AOD and ln λ can be represented successfully with a quadratic function. Taking into account the AODs at 340, 380, 500 and 1020 nm and a second order curve fit, the coefficients fulfilling the following relationship were obtained

$$\ln \tau_a = a_0 + a_1 \ln \lambda + a_2 (\ln \lambda)^2 \quad (5)$$

Eck et al. (2001) excluded wavelength of 1020 nm in the derivation due to a potential weak signal from water vapor absorption near this wavelength and, instead, included 870 nm. Following the methodology applied by Eck et al. (1999), we included 1020 nm, since it was the only channel that our sunphotometers have in the infrared. Consequently, discarding 1020 nm would have required deriving the exponent from the UV (340 and 380 nm) and visible (500 nm) wavelengths without any component in the near infrared which would introduce large errors in the derivation.

3. Results and discussion

Global irradiance mean and standard deviation for clear days between March 15th and October 18th, 2011, separated in two groups, before and after the eruption, were calculated for LPh (Fig. 3). While, at 380 nm (Fig. 3c), values before and after the eruption showed almost no difference, at 320 and 305 nm, they exhibited a decrease, which was more pronounced at the lowest wavelength (around 40% decrease, at SZA 45°). As explained in Section 2.1, the variation, at 305 nm, reflects not only changes in AOD, but also in ozone.

The variation in global irradiance, at 320 and 380 nm, for pair of days obtained comparing all days before with all days after the eruption and grouped in 1° SZA are shown in Fig. 4a and c. Large dispersion was observed at both wavelengths. Mean values and standard deviations calculated, at 5° SZA intervals, showed small and not statistically significant decrease at 380 nm, while, at 320 nm, the mean decrease was near 10% (SZA $\leq 60°$). With the aims of determining if this result was real, and not a consequence of compensation between AOD and albedo variations, the analysis was repeated for 1999, when no eruption or any other event that could have produce major changes in AOD occurred. Results are

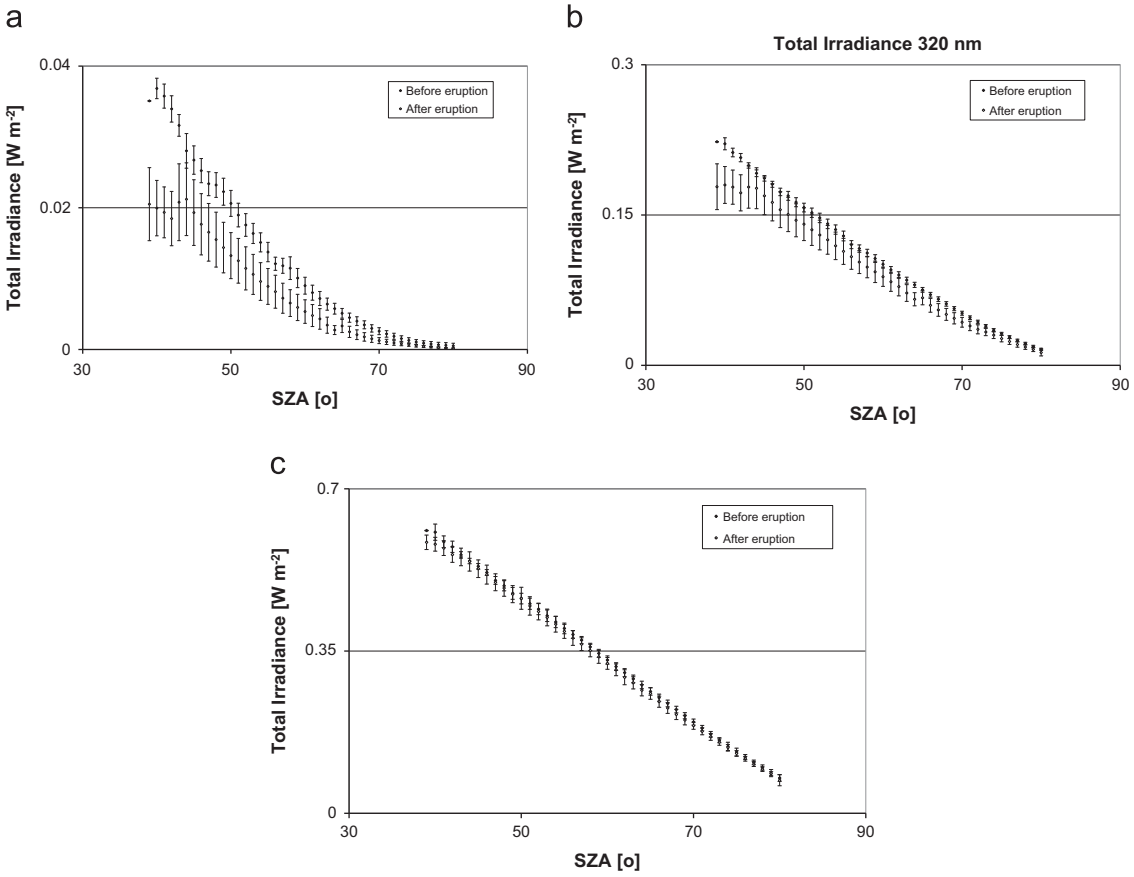

Fig. 3. Global irradiance mean and standard deviation for clear sky days. Before (black diamonds) and after (empty diamonds) the eruption of the Puyehue-Cordon Caulle, grouped in 1° SZA, (a) 305 nm, (b) 320 nm and (c) 380 nm.

shown in Fig. 4b and d, where it was observed that, the difference between clear days of both groups (March 15th to May 5th and September 15th to October 18th) was not statistically significant, neither at 320 nor at 380 nm, although less variability was exhibited during 1999 than in 2011. From these results, it may be concluded that the eruption resulted in an increased in the variability at both wavelengths with a decrease in global irradiance near 10% at 320 nm, but not statistically significant decrease in mean global irradiance, at 380 nm.

At 305 nm, the effect of aerosols and ozone are combined. As consequence of seasonality, the total column ozone for days before the volcano eruption was 265 ± 15, and 315 ± 26 after the eruption. After identifying days with equal or very closed TOC, two groups were obtained, 19 Sep (288 DU) – 27 Mar (292 DU) and 18 Oct (257 DU) – 5 Apr (256 DU) – 1 May (257 DU). Variation in global irradiance at 305 nm was calculated for both groups, and the results are shown, in Fig. 5a. A decrease between 19 and 28% ($SZA < 60^\circ$) was observed between pairs of days with one after and one before the volcano eruption, while the difference between a pair with both days before the volcano eruption (April 5th and May 1st) was $\leq 5\%$ (Fig. 5a). The same methodology was applied to data 1999. Total ozone column for clear days before June 4th was 258 ± 14 and 308 ± 13 DU, for clear days after June 4th. In 1999, only one pair of days was identified with the same total ozone column: 24 Mar (280 DU) and 29 Sep (281 DU). When calculating the variation, the result was closed to the result observed in 2011, for pair of days with both days before the eruption (Fig. 5b).

With the aims of increasing the size of our sample, we modeled the global irradiance at SZA 45, 50, 55 and 60°, for the selected clear days before and after the eruption (June 4th), and calculated the difference consequence of ozone changes in pair of days with one before and one after June 4th. Then, this value was subtracted from the difference in the measured irradiance, at the same SZA as modeled $\pm 0.1^\circ$, obtaining the change produced by AOD, as explained in Section 2.1. For 2011, large dispersion was observed in the resulting values, consistent with the results observed at 380 nm, but at 305 nm, all values were negative (Fig. 5a, small dots). For SZA smaller than 60°, the decrease was $-18 \pm 8\%$, similar to the result obtained comparing days with the same TOC. When repeating this procedure for 1999, the mean variation was small and not statistically significant. (-2.3 ± 3.8, $SZA \leq 60^\circ$) (Fig. 5b), indicating that in absence of the eruption there was not significant difference in days before and after June 4th, once correcting for ozone changes, hence the hypothesis that change in albedo could compensate changes in AOD can be discard. Smaller dispersion in 1999 than in 2011 was also observed, as pointed out when analyzing 380 nm.

There is not AERONET data at the region of the NHNP and the closest station is more than 500 km away. Then, the only AOD data available was obtained during the campaigns. Fig. 6 shows AOD and Angstrom exponent diurnal variabiliry and daily mean, for the three sites, at 380 nm, during the 2010 campaign. Fig. 7 shows the same parameters for the campaign 2011. In addition, AOD and Angstrom exponent obtained on September 14th, 2011 between 14:13 and 15:53 UT, at Puerto Pañuelo (Fig. 1), were included.

For most days, AOD and Angstrom exponent showed large diurnal variability, even for 2010 (Figs. 6 and 7). An inverse relation was observed between this parameters, indicating that increases in AOD correspond to an increase in coarse particles.

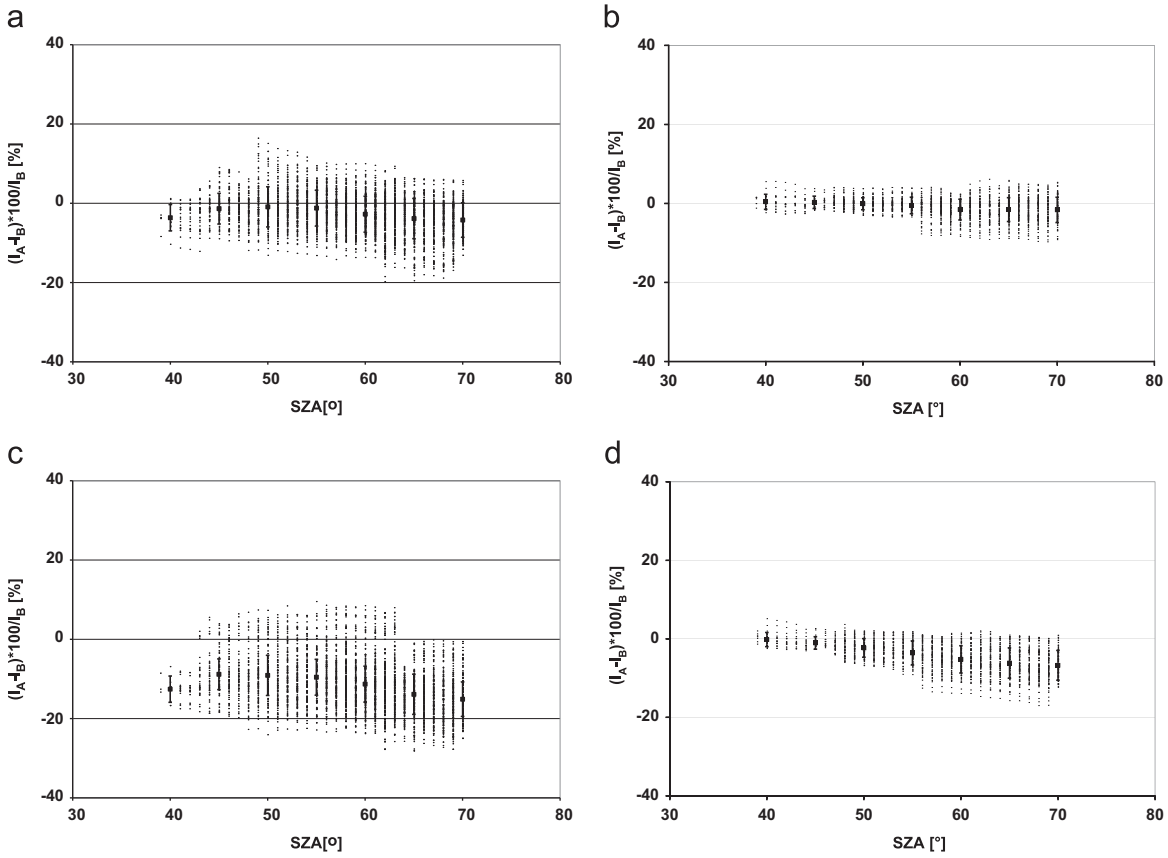

Fig. 4. Variation in global irradiance, at 320 and 380 nm. Values were obtained comparing all clear days before and after June 4th and were grouped in 1° SZA. Mean values (squares) and standard deviation calculated in 5° SZA intervals are also included, (a) 380 nm, 2011 and (b) 380 nm, 1999, (c) 320 nm, 2011 and (d) 320 nm, 1999.

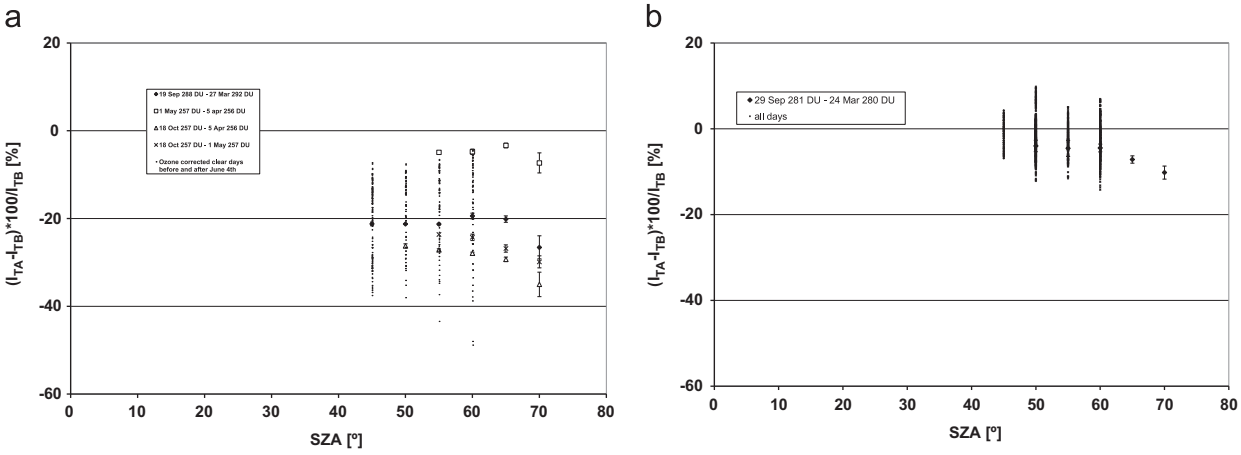

Fig. 5. Variation in global irradiance at 305 nm. Values were obtained comparing clear days before and after June 4th, with equal or similar TOC and all days, once removing the variation produced by ozone changes.

At LPh, AOD observed during 2011 did not differ considerably from those measured during 2010, except for September 18th, when AOD were around twice larger than the mean value observed in 2010. Nevertheless, the Angstrom exponent exhibited lower values for all days during the campaign 2011, compared to 2010, particularly for September 18th, indicating the presence of larger particles (Figs. 6b and 7b). Mt Catedral, at higher altitude, showed similar results, although the changes were much less pronounced. The AOD observed at Puerto Pañuelo, on September 14th, was even larger than the AOD observed at LPh, on September 18th (Fig. 7a and g). Also, the Angstrom exponent was smaller (Fig. 7b and h), indicating the presence of larger particles.

Analyzing the sequence September 14th to September 18th, large variability in the aerosols load was observed. The AOD measured at Puerto Pañuelo, on September 14th, was large and the Angstrom exponent was small, indicating the presence of coarse particles. September 15th was a rainy day and, on September 16th and 17th, the AOD was relatively low (values similar to 2010) and the Angstrom exponent indicated the presence of smaller particles. This would indicate that the ash load present on September 14th was

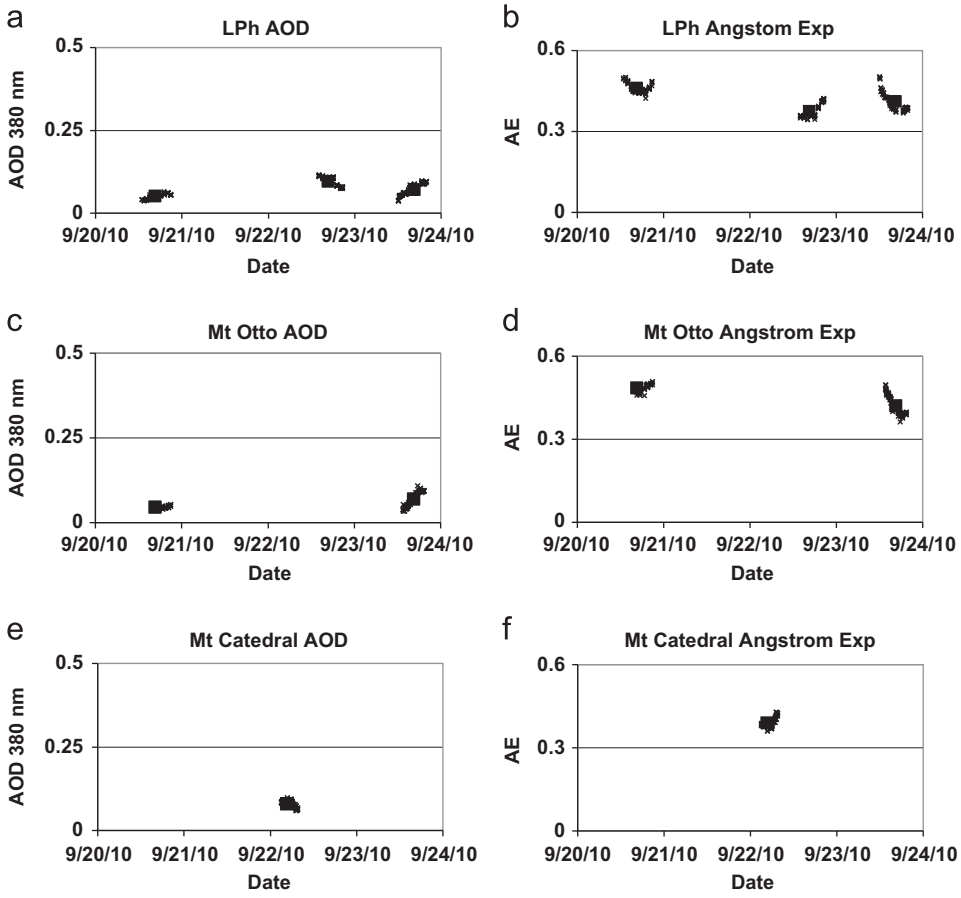

Fig. 6. Aerosol optical depth and Angstrom exponent. Diurnal variation and daily mean for 2010. Angstrom exponent was calculated applying least squares to the exponents obtained from AOD at the wavelength pairs 380–340 nm, 500–380 nm and 1020–500 nm (Eck et al., 1999).

partially cleaned by the rain. Finally, on September 18th, a change in wind intensity and direction produced an increase in AOD and particle size, rising AOD at LPh twice. Although it is a small sample, this sequence would explain the large variability observed in global irradiance after the eruption.

Variation in direct irradiance, at 380 nm, at LPh, is shown in Fig. 8. Two well defined groups of values were observed, as consequence of AOD changes. One group, obtained when comparing direct irradiance on 16th and 17th of September, 2011 with clear days in the campaign 2010, presented from a slight increase to near 10% decrease (SZA=45°), and the other group, resulting from comparing September 18th with clear days in the campaign 2010, exhibited a decrease between 21 to 30% (SZA=45°). In both groups, an increase in the absolute value is observed as SZA increases. Comparing Fig. 4a and Fig. 8, the effect of the eruption seemed to be more pronounced on the direct than in the global irradiance, although the compared irradiance do not belong exactly to the same time periods (2011 before and after the eruption and September 2010 and 2011, respectively), although data of the campaign 2011 was included in Fig. 4a. This difference between the decrease in global and direct irradiance could be expected, since the increase produced in the amount of particles present in the atmosphere would produce an increase in the diffuse which would partially compensate the decrease in the direct, resulting in smaller decrease in the global irradiance, than in the direct. This result was, then, confirmed when analyzing data obtained at Mt Otto and Mt Cathedral.

In order to evaluate the effect of the eruption at different altitudes, we studied data at Mt Otto (1386 msl) and Mt Catedral (1930 msl). Total ozone column for clear sky days during the campaigns is shown in Table 2.

Clear sky measurements at Mt Otto were obtained on September 20th and 23rd, 2010 and September 16th, 2011. Total ozone column was similar for the three days (329, 325 and 323 DU, respectively). The AOD, in 2011, did not show significant difference regarding to values observed in 2010, at 380 nm (Fig. 6c and Fig. 7c), although Figs. 6d and 7d indicated the presence of larger particles, in 2011. Global irradiance, at 380 nm, showed smaller variation than the direct, particularly for September 16th–September 20th. When analyzing global irradiance, at 305 nm, after applying the correction for ozone, a decrease was observed for both pair of days, which was not in agreement with the variation observed in AOD at 380 nm (Table 3 and Figs. 6c and 7c), indicating that the aerosol load was different at 380 than at 305 nm. This result would be consequence of the presence of fine particles, SO_2. When considering both pairs of days, only the result for global irradiance, at 305 nm, was statistically significant, with a mean decrease of almost 12%. This value was smaller than the average observed at LPh when comparing days before and after June 4th (Fig. 5a), but no one of the days observed at Mt Otto, during 2011, included large AOD at 380 nm. Daily AOD, Angstrom exponent and direct irradiance showed small difference between LPh and Mt Otto, when comparing the same set of days (Figs. 6 and 7, and Table 3).

Results for Mt Cathedral are shown in Table 4. Clear sky measurements were performed on September 22nd, 2010 and September 17th and 18th, 2011. While AOD, at 380 nm, was slightly lower on September 17th, 2011 than on September 22nd, 2010, on September

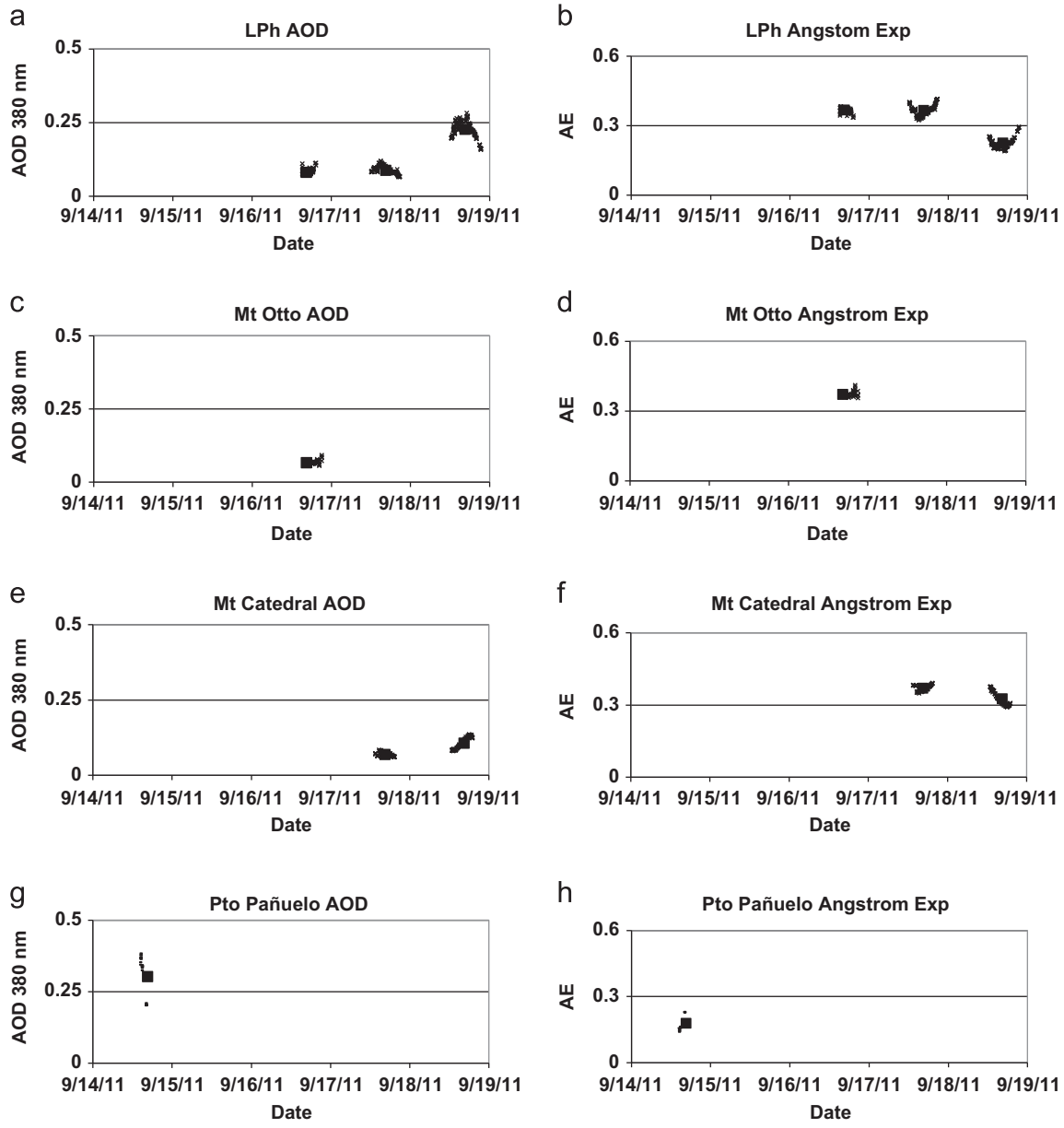

Fig. 7. Aerosol optical depth and Angstrom exponent. Diurnal variation and daily mean for 2010. Angstrom exponent was calculated applying least squares to the exponents obtained from AOD at the wavelength pairs 380–340 nm, 500–380 nm and 1020–500 nm (Eck et al., 1999).

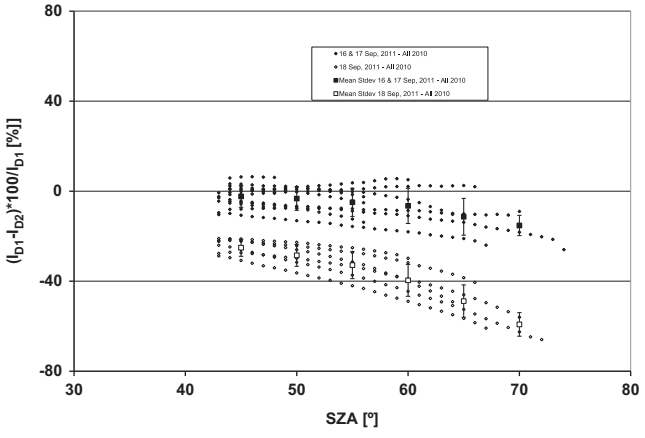

Fig. 8. Variation in direct irradiance at the Laboratory of Photobiology. Comparing values for September 2011 and 2010, at 380 nm.

Table 2
Total ozone column for clear days during the campaigns performed in September 2010 and 2011.

Day 2010	TOC [DU]	Day 2011	TOC [DU]
20-Sep	329	16-Sep	323
22-Sep	341	17-Sep	267
23-Sep	325	18-Sep	283

18th, it was higher. Both days, (17th and 18th) exhibited lower AOD at Mt Catedral than at LPh, but for the 18th, the difference was much larger. As a result, when comparing September 17th and September 22nd, there was a slight increase in direct irradiance at Mt Catedral, while comparing September 18th with September 22nd, there was a decrease (-4.4 ± 2.7), but much smaller than the decreased observed at LPh (-27 ± 4.8) on the same pair of days. Global irradiance at 380 nm showed results in the range of the variability observed before the eruption, while at 305 nm, both pair of days exhibited a decrease,

Table 3
Variation in global irradiance between 2010 and 2011, at Mt Otto and, in direct irradiance, at Mt Otto and LPh (SZA ≤ 60°).

Days	Mt Otto			LPh
	Global 305 nm correct Oz [%]	Global 380 nm [%]	Direct 380 nm [%]	Direct 380 nm [%]
9/16/11–9/20/10	−16.3 ± 2.4	−3.5 ± 0.4	−7.4 ± 2.4	−7.7 ± 2.7
9/16/11–9/23/11	−6.3*/−1.5	4.2 ± 1.2	4.8 ± 0.8	n.s.
All	−11.7 ± 5.4	n.s.	n.s.	n.s.

Table 4
Variation in global irradiance between 2010 and 2011, at Mt Catedral and, in direct irradiance, at Mt Catedral and LPh (SZA ≤ 60°).

Days	Mt Catedral			LPh
	Global 305 nm correct Oz [%]	Global 380 nm [%]	Direct 380 nm [%]	Direct 380 nm [%]
9/17/11–9/22/10	−8.5 ± 3.6	n.s.	3.2 ± 1.0	n.s.
9/18/11–9/22/10	−13.4 ± 3.3	−2.9 ± 2.0	−4.4 ± 2.7	−27.1 ± 4.8
All	−10.9 ± 4.2	n.s.	n.s.	n.s.

Table 5
Variation in AOD, global and direct irradiance between September 17th and 18th, 2011, at LPh and Mt Catedral (SZA ≤ 60°).

Site	Global 305 nm correct Oz [%]	Global 380 nm [%]	Direct 380 nm [%]	AOD 380 nm [%]
Laboratory of Photob.	−4.6	−5.6	−27.1	156
Mt Catedral	−3.2	−4.4	−7.6	52

although larger for September 18th–September 22nd (−8.5 ± 3.6 and −13.4 ± 3.3%). In the average, not statistically significant results were observed, except for global irradiance at 305 nm, which presented near 11% decrease. These results showed agreement with the analysis for Mt Otto, since smaller effect of the eruption was observed in the global UV-A irradiance than in the direct, while at the UV-B, a decrease was observed at the first pair of days, even when AOD at 380 nm decreased. Comparing Table 4 and Fig. 7a and e, it was observed that under large aerosol load, larger difference in AOD and direct irradiance were observed at LPh than at Mt Catedral. This result is consistent with the presence of coarse particles at lower altitude (LPh), which usually were not present at higher altitude.

Global irradiance, at 305 nm, exhibited slightly larger mean decrease at Mt Otto (1386 msl) than at Mt Catedral (1930 msl), even though that no one of the analyzed days presented large AOD at 380 nm, at Mt Otto. From the comparison between Mt Catedral and LPh, it may be inferred that if large AOD at 380 nm would have been observed, then, the decrease at 305 nm would have been much larger at Mt Otto than at Mt Catedral.

Comparing September 18th with September 17th, at LPh and at Mt Catedral the relative variation in all the studied parameters could be analyzed (Table 5). It was observed that the increase in AOD and decrease of direct irradiance was much more pronounced at LPh than al Mt Catedral, while the decrease in global irradiance at the UV-B and UV-A was only slightly lower at Mt Cathedral. Nevertheless, it should be taken into account that the decrease at 305 nm, in Table 5, was indeed superimposed to a baseline decrease, which seemed to be smaller at Mt Catedral than at LPh.

4. Conclusions

As a result of the eruption, mean global irradiance at 380 nm, did not show statistically significant decrease at any site. Although, more variability was observed, compared to 1999, when no eruption or any other event that could have produced major changes in AOD occurred. Also, in particular days, under large aerosol load, a decrease was observed in 2011, which was slightly larger at the lower altitude site.

Global irradiance, at 305 nm, exhibited a mean decrease near 20%, after the eruption, at the Laboratory of Photobiology (804 msl) while at 320 nm, the decrease was closed to 10%. Larger variability than in year 1999 was also observed at both wavelengths, in agreement with the results for 380 nm. These results indicated that the eruption affected more to lower wavelengths in the UV with a decreasing effect as wavelength increased, and, in addition, incremented the variability at all wavelengths.

At 305 nm, a decrease was detected at all sites, even in days when AOD 380 nm did not show difference regarding to 2010, this would be the consequence of the presence of fine particles (SO_2). The decrease was larger when AOD at 380 nm increased and at the lower altitude site, due to the presence of coarse particles.

During the campaign 2011, daily mean AOD exhibited larger variability than in 2010, with days presenting values similar to 2010 and days with larger AOD. Under large aerosol load, the increase was larger at the lower altitude site. Coarse particles would be the responsible for this situation.

The effect of the eruption was more pronounced in the direct irradiance than in the global irradiance, at 380 nm. This difference could be expected, since the increase produced in the amount of particles present in the atmosphere would produce an increase in the diffuse which would compensate, in part, the decrease in the direct, resulting in smaller decrease in the global irradiance. The difference was much larger at lower altitude, where more coarse particles were present.

AOD, Angstrom exponent and direct irradiance showed small difference between LPh and Mt Otto.

Since, for year 2011, clear days closest to the beginning of the eruption were at about the same date as the campaign 2011, the results reported in this analyzes reflect the situation between three and four and half month after the eruption started. Probably, the decrease in irradiance was larger at the beginning of the eruption.

The observed results would indicate that, for several months, ecosystems might have been affected by the observed changes. The spectral dependence in the decrease in global irradiance would result in more pronounced effect on those biological functions that are more sensitive to lower wavelengths (i.e.: vitamin D photoconversion; Bouillon et al., 2006), than on those exhibiting a flatter action spectrum (i.e.: phytoplanction production; Neale and Kieber, 2000). Also, ecosystems living at lower altitude would have resulted more affected than those at higher altitude.

Acknowledgements

This work was supported by the Agencia Nacional de Promocion Cientifica y Tecnologica (ANPCyT), Argentina (PICT2007 N00377). Additional fundings for data collection and analysis was provided by Argentina's Consejo Nacional de Investigaciones Cientificas y Tecnicas (CONICET). The authors want to thank the Japanese International Cooperation Agency (JICA) for having provided the radiometer used at the movil station. The authors are thankful to NASA, Jeff Schmaltz and Holli Riebeek, LANCE/EOSDIS MODIS Rapid Response Team at NASA GSFC, for MODIS images. We also thank to Mrs Mariana Reissig for drawing the zonal map from a satellite image. The authors wish to thank Mr. Rocky Booth, Mr.

Jim Ehramjian and the UV group (Biospherical Instruments Inc.) for the calibration of the reference GUV. Ozone data used in this effort were acquired as part of the activities of NASA's Science Mission Directorate, and are archived and distributed by the Goddard Earth Sciences (GES) Data and Information Services Center (DISC). We also want to thank the technical and scientific bureau of Nahuel Huapi National Park, who granted the permissions for the measurements inside different areas of the Park; Alta Patagonia, Refugio Lynch and their personnel, who provided the logistics required during the campaigns performed at Mount Catedral; and Fundación S.M. Furhman and their personnel, who made possible the transportation and measurements at Mount Otto. We are grateful to Laboratory of Photobiology (INIBIOMA, Universidad Nacional del Comahue) and its personnel, for their support during data collection.

References

Angstrom, A., 1929. On the atmospheric transmission of sun radiation and on dust in the air. Geogr. Ann 12, 130–159.

Ansmann, A., Tesche, M., Seifert, P., Groß, S., Freudenthaler, V., Apituley, A., Wilson, K.M., Serikov, I., Linné, H., Heinold, B., Hiebsch, Schnell, A.F., Schmidt, J., Mattis, I., Wandinger, U., Wiegner, M., 2011. Ash and fine mode particle mass profiles from EARLINET-AERONET observations over central Europe after the eruptions of the Eyjafjallajökull volcano in 2010. J. Geophys. Res. 116, http://dx.doi.org/10.1029/2010JD015567 (D00U02).

Bekki, S., Bodeker, G.E., 2010, Future Ozone and Its impact on surface UV, in WMO (World Meteorological Organization), Scientific Assessment of Ozone Depletion: 2010, Global Ozone Research and Monitoring Project-Report No. 50, 572 pp., Geneva, Switzerland.

Booth, R., 1998. Application Note: Temperature Coefficients in PUV and GUV Radiometers and Suggested Compensation Methods, Biospherical Instruments Inc.

Booth, R., Mestechkina, T., Morrow, J.H., 1994. Errors in the reporting of solar spectral irradiance using moderate band-width radiometers and experimental investigation. In: J.S. Jaffe. (Ed.), Ocean Optics XII, Proceedings of SPIE, 2258, pp. 654–663.

Bouillon, R., Eisman, J., Garabedian, M., Holick, M., Kleinschmidt, J., Suda, T., Terenetskaya, I., Webb, A., 2006. Action Spectrum for the Production of Previtamin D3 in Human Skin. UDC: 612.014.481-06, CIE, Vienna.

Chubarova, N.Y., Krotkov, N.A., Geogdzhaev, I.V., Kondranin, T.K., Khattatov, V.U., 1997. Spectral UV irradiance: the effects of ozone, cloudiness and surface albedo. In: Smith and Stamnes. (Eds.), Proceedings of IRS'96 Current problems in Atmospheric Radiation. A Deepak Publishing 1997, Hampton Meeting, Fairbanks.

Dahlback, A., 1996. Measurements of biologically effective UV doses, total ozone abundance and cloud effects with multi-channel moderate bandwidth filter instruments. Appl. Opt 35, 6514–6521.

Diaz, S., Booth, C.R., Armstrong, R., Brunat, C., Cabrera, S., Camilion, C., Cassiccia, C., Deferrari, G., Fuenzalida, H., Lovengreen, C., Paladini, A., Pedroni, J., Rosales, A., Zagarese, H., Vernet, M., 2005. Multi-channel radiometers calibration. A new approach. Appl. Opt. 44 (26), 5374–5380.

Díaz, S.B., Booth, C.R., Lucas, T.B., Smolskaia, I., 1994. Effects of ozone depletion on irradiances and biological doses over Ushuaia, impact of UV-B radiation on pelagic freshwater ecosystems. In: Williamson, C.E., Zagarese, H.E. (Eds.), Archive Fur Hydrobiologie, 43. Ergebnisse de Limnologie, pp. 115–122.

Diaz, S., Camilion, C., Deferrari, G., Fuenzalida, H., Armstrong, R., Booth, C., Paladini, A., Cabrera, S., Casiccia, C., Lovengreen, C., Pedroni, J., Rosales, A., Zagarese, H., Vernet, M., 2006. Ozone and UV radiation over southern South America: climatology and anomalies. Photochem. Photobiol. 2006 (82), 834–843.

Díaz, S., Nelson, D., Deferrari, G., Camilión, C., 2003. A model to extend spectral and multi-wavelength UV irradiances time series. Model development and validation. J. Geophys. Res. Atmos 108 (D4), 4150, http://dx.doi.org/10.1029/2002JD002134.

Diaz, S.B., Paladini, A.A., Braile, H.G., Dieguez, M.C., Deferrari, G.A., Vernet, M., Vrsalovic, J., 2013. Effect on Irradiance of the eruption of the Cordon Caulle (Chile) at different altitudes in the Nahuel Huapi National Park (Patagonia, Argentina). In: Diofantos G. Hadjimitsis, Kyriacos Themistocleous, Silas Michaelides, George Papadavid. (Eds.), First International Conference on Remote Sensing and Geoinformation of the Environment (RSCy2013), Proceedings of SPIE 8795, 879512.

di Sarra, A., Cacciani, M., Chamard, P., Cornwall, C, DeLuisi, J.J., Di Iorio, T., Disterhoft, P., Fiocco, G., Fua, D., Monteleone, F., 2002. Effects of desert dust and ozone on the ultraviolet irradiance at the Mediterranean island of Lampedusa during PAUR II. J. Geophys. Res. 107 (D18), 8135 (doi:1029/2000JD000139).

Eck, T.F., Holben, B.N., Dubovik, O., Smirnov, A., Slutsker, I., Lobert, M., Ramanathan, V., 2001. Column-integrated aerosol optical properties over the Maidives during the northeast monsoon for 1998–2000. J. Geophys. Res. 106 (D22), 28,555–28,566 (27).

Eck, T.F., Holben, B.N., Reid, J.S., Dubovik, O., Smirnov, A., O'Neill, N.T., Slutsker, I., Kinne, S., 1999. Wavelength dependence of the optical depth of biomass burning, urban, and desert dust aerosols. J. Geophys. Res. 104 (D24), 31,333–31,349.

Estupinan, J.G., Raman, S., Crescenti, G.H., Streitcher, J.J., Barnard, W.F., 1996. The effects of clouds and haze on UV-B radiation. J. Geophys. Res. 101 (16), 807–816.

Frederick, J.E., Diaz, S.B., Smolskaia, I., Esposito, W., Lucas, T., Booth, C.R., 1994. Ultraviolet solar radiation in the high latitudes of South America. Photochem. Photobiol. 60, 356–362.

Frederick, J., Steele, H., 1995. The transmission of sunlight through cloudy skies: an analysis based on standard meteorological information. J. Appl. Meteorol. 34, 2755–2761.

Kirchhoff, V.W., Silva, A.A., Costa, C.A., Paes Leme, N., Pavao, H.G., Zaratti, F., 2001. UV-B optical thickness observations of the atmosphere. J. Geophys. Res. 106, 2963–2973.

Lubin, D., Frederick, J., 1989. Measurements of enhanced springtime ultraviolet springtime radiation at Palmer station. Geophys. Res. Lett 16 (8), 783–785.

McArthur, L.J.B., Fioletov, V.E., Kerr, J.B., McElroy, C.T., Wardle, D.I., 1999. Derivation of UV-A irradiance from pyranometer measurements. J. Geophys. Res. 104, 30139–30151.

McKenzie, R., Bodeker, G., Scott, G., Slusser, J., Lantz, K., 2006. Geographical differences in erythemally-weighted UV measured at mid-latitude USDA sites. Photochem. Photobiol. Sci. 5 (3), 343–352, http://dx.doi.org/10.1039/B510943D.

McKenzie, R.L., Weinreis, C., Johnston, P.V., Liley, B., Shiona, H., Kotkamp, M., Smale, D., Takegawa, N., Kondo, Y., 2008. Effects of urban pollution on UV spectral irradiances. Atmos. Chem. Phys. 8 (18), 5683–5697, http://dx.doi.org/10.5194/acp-8-5683-2008.

Mc Peters, R., Beach, E., 2013. AURA OMI, NASA/GSFC, version 8.5. URL: ⟨ftp://toms.gsfc.nasa.gov/pub/omi/data/overpass/⟩.

Michalsky, J., Denn, F., Flynn, C., Hodges, G., Kiedron, P., Koontz, A., Schlemmer, J., Schwartz, S.E., 2010. Climatology of aerosol optical depth in north & central Oklahoma: 1992–2008. J. Geophys. Res. 115, D07203, http://dx.doi.org/10.1029/2009JD012197.

Morys, M., Mims III, F.M., Hagerup, S., Anderson, S.E., Baker, A., Kia, J., Walkup, T., 2001. Design, calibration, and performance of MICROTOPS II handheld ozone monitor and Sun photometer. J. Geophys. Res. Atmos. 106 (D13), 14,573–14,582, http://dx.doi.org/10.1029/2001JD900103.

NASA, 2013a. ⟨http://www.nasa.gov/topics/earth/features/20110615-volcano.html⟩.

NASA, 2013b. ⟨http://www.nasa.gov/topics/earth/features/20110615-volcano.html⟩ Image Courtesy Jeff Schmaltz, LANCE/EOSDIS MODIS Rapid Response Team at NASA GSFC. Caption by Holli Riebeek.

Neale, N.J., Kieber, D.J., 2000. Assessing biological and chemical effects of UV in the marine environment: spectral weighting functions. In: Hester, R.E., Harrison, R. M. (Eds.), Causes and Environmental Implications of Increased UV-B Radiation. Royal Society of Chemistry, Cambridge, pp. 61–84.

SERNAGEOMIN, 2013. Reporte Especial de Actividad Volcánica No 122 Complejo Volcánico Puyehue—Cordón Caulle., ⟨http://www.sernageomin.cl/volcan.php?pagina=6&id=38⟩.

Skouratov, S., 1997. Influence of the Pinatubo eruption on the aerosol optical depth in the Arctic in the summer of 1993. Atmos. Res. 44, 125–132.

SPARC (Stratospheric Processes And their Role in Climate), 2006. Assessment of Stratospheric Aerosols Properties. L. Thomason and Th. Peter. (Eds.), SPARC Report No. 4, WCRP-124, WMO/TD-No. 1295.

Stamnes, K., Tsay, S.C., Wiscombe, W., Jayaweera, K., 1990. Numerically stable algorithm for discrete-ordinate-method radiative transfer in multiple scattering and emitting layered media. Appl. Opt. 27, 2502–2509.